

Neutron irradiation effects on electrical properties and deep-level spectra in undoped *n*-AlGaIn/GaN heterostructures

A. Y. Polyakov,^{a)} N. B. Smirnov, A. V. Govorkov, and A. V. Markov
Institute of Rare Metals, B. Tolmachevsky 5, Moscow 119017, Russia

S. J. Pearton
Department of Materials Science and Engineering, University of Florida, 132 Rhines Hall, Gainesville, Florida 32611

N. G. Kolin, D. I. Merkurisov, and V. M. Boiko
Obninsk Branch of Federal State Unitary Enterprise, Karpov Institute of Physical Chemistry, 249033 Obninsk, Kaluga region, Kiev Avenue, Russia

(Received 30 March 2005; accepted 30 June 2005; published online 11 August 2005)

The effect of neutron irradiation on the electrical properties of undoped *n*-AlGaIn/GaN heterostructures is reported. The two-dimensional electron-gas (2DEG) mobility starts to decrease at neutron doses above 10^{14} cm⁻², while the 2DEG concentration slightly increases at low doses and decreases dramatically for doses higher than 2.5×10^{16} cm⁻². The result is that the mobility/concentration product (a figure of merit for transistors) starts to decrease appreciably after the dose of 10^{15} cm⁻². Capacitance-voltage and admittance spectroscopies, indicate that tunneling of electrons into the states near $E_c - 0.21$ eV in AlGaIn is a serious factor when cooling down the virgin or lightly irradiated samples. For heavily irradiated samples the states in AlGaIn are close to 0.3 and 0.45 eV, respectively, from the bottom of the conduction band. Deep-level spectroscopy measurements reveal the presence of hole traps with apparent activation energies of 0.18 and 0.21 eV for lightly irradiated samples and deeper hole traps with activation energies of 0.6 and 1 eV in heavily irradiated samples. © 2005 American Institute of Physics. [DOI: 10.1063/1.2006223]

I. INTRODUCTION

AlGaIn/GaN heterojunctions are of great interest for use in high electron mobility transistor (HEMT) structures due to strong polarization effects leading to a very high two-dimensional electron-gas (2DEG) density at the AlGaIn/GaN interface.^{1,2} Very promising results have been demonstrated for microwave AlGaIn/GaN HEMTs operating at high power levels of ~ 10 W/mm, at high frequencies of ~ 10 GHz, and very high temperatures of ~ 400 °C.^{1,2} Some of the applications that are being pursued with such devices require them to remain operable when subjected to irradiation with protons, electrons, γ rays, or neutrons. There has been considerable effort to understand the nature of radiation defects in group-III nitrides and GaN-based heterojunctions. The most detailed studies have been performed for electron and proton irradiation of *n*-GaN.³⁻⁹ Such irradiation mostly introduces relatively shallow electron traps near 0.07, 0.2, and 0.3 eV from the conduction-band edge³⁻⁹ and the 0.07-eV traps were identified as nitrogen vacancies.⁴ Deeper electron traps near 0.7 and 0.9 eV from the conduction band were observed after treatment with heavier ions (He, N) (Refs. 9 and 10) or with higher proton doses.⁷ The formation of deep hole traps near $E_v + 0.25$ eV, $E_v + 0.4$ eV, $E_v + 0.6$ eV, and $E_v + 0.9$ eV has been reported in proton-irradiated *n*-GaN (Ref. 7) and *p*-GaN (Ref. 11) samples. The 0.7-eV electron traps and the 0.6-eV hole traps were sug-

gested as possible lifetime-killer defects.⁷ In *p*-AlGaIn (Ref. 12) and *n*-AlGaIn (Ref. 9) with a low Al mole fraction of 0.12–0.2, the defects introduced by proton implantation were similar to those in *n*-GaN and *p*-GaN. In *n*-AlGaIn samples with higher AlN mole fraction of ~ 0.4 , the 100-keV proton implantation could increase the resistivity of the layers by up to five orders of magnitude, depending on the proton dose.¹³ When compared to other III-V materials, GaN showed a higher radiation hardness.^{5,6,9} Typically, in moderately doped *n*-GaN, serious changes of electron concentration and mobility after proton or electron implantation started at doses $> 10^{14}$ cm⁻². Radiation defects usually could be annealed at temperatures below 500 °C,^{6,9} but defects responsible for reduced lifetimes were reported to persist to ~ 800 °C.⁷ The degradation depends strongly on the energy of the incident particles and not just on fluence.

Much less has been done to study the effects of neutron irradiation on GaN. For neutron irradiation of *n*-GaN thin films and Schottky diodes prepared by magnetron sputtering,¹⁴ measurable changes of electrical properties occur for doses $> 10^{14}$ cm⁻². Some work has also been reported for radiation defects in AlGaIn/GaN HEMTs (Refs. 15–26) and GaN-based light-emitting diodes.^{26–29} The results were mostly devoted to proton and γ irradiation. The 40-MeV proton implantation of MgO or Sc₂O₃-passivated AlGaIn/GaN HEMTs with doses of 5×10^9 – 5×10^{10} cm⁻² led to very slight (about 30% after the higher dose) changes of device characteristics.^{15,16} Cai *et al.*²⁴ observed a 70% decrease in AlGaIn HEMTs transconductance after irradiation with 10^{14} cm⁻² of 1.8-MeV protons. Luo *et al.*²⁵ reported

^{a)}On leave from the Department of Materials Science and Engineering, Carnegie Mellon University, Pittsburgh, Pennsylvania 15213-3890.

| |
|---|
| 200 Å UID $\text{Al}_{0.2}\text{Ga}_{0.8}\text{N}$ cap |
| 200 Å $\text{Al}_{0.2}\text{Ga}_{0.8}\text{N}:\text{Si}$, $\sim 10^{18} \text{ cm}^{-3}$ |
| 30 Å UID $\text{Al}_{0.2}\text{Ga}_{0.8}\text{N}$ spacer |
| ~ 200 Å 'transition' GaN |
| $\sim 1.0 \mu\text{m}$ UID GaN buffer |
| ~ 200 Å LT AlN |
| (0001) Sapphire |

FIG. 1. Schematic of the AlGaIn/GaN heterostructure sample used in these experiments.

that, with Co^{60} γ irradiation, measurable changes of HEMT characteristics occurred after doses exceeding 300 Mrad. All these changes in device performance were explained by the formation of deep traps compensating conductivity, but the nature of the traps and their location in the heterojunction were not studied in detail. Little is known about the effects of neutron irradiation on AlGaIn heterojunctions. In this paper we present studies of 2DEG properties as affected by neutron irradiation and show that traps both in the AlGaIn barriers and in the GaN channel play a role in the observed changes.

II. EXPERIMENT

The AlGaIn/GaN heterojunctions were grown by metal-organic chemical-vapor deposition (MOCVD) on sapphire. Both the GaN and the AlGaIn layers were nominally undoped. The thickness of the AlGaIn barrier layer was 40 nm and the Al mole fraction was close to $x=0.3$. The GaN buffer layer was grown on an AlN low-temperature nucleation buffer and was 1 μm thick. A schematic of the structure is shown in Fig. 1.

The samples were irradiated at room temperature by fast (1 MeV) neutrons in the WWR-c-type nuclear reactor of the Obninsk branch of the Karpov Institute. The doses used were 10^{13} , 10^{14} , 10^{15} , 2.5×10^{16} , and $1.7 \times 10^{17} \text{ cm}^{-2}$. The nonionizing energy loss (NIEL) of 1-MeV neutrons is $<1 \text{ eV/particle}$ based on stopping and range of ions in matter (SRIM) simulations.³⁰ The samples were examined 1 week after the irradiations were completed. We did not observe any significant annealing effects on this time scale on remeasured samples. The high end of the doses used here is generally well in excess of those studied previously in GaN structures and allows us to see the range over which the degradation in material properties is linear with dose. It would be expected that as the radiation accumulates, defect clustering may become more significant and the material may no longer show a linear response to dose. The high end of the dose range also enables us to get a better appreciation for the radiation hardness of AlGaIn/GaN to high total neutron doses. Before and after the irradiation of the 2DEG, concentration and mobility were measured at room tempera-

ture and at 77 K by Hall (magnetic field of 5000 G) and van der Pauw techniques using In Ohmic contacts. The carrier-concentration profiles were established by capacitance-voltage (C - V) measurements at temperatures between 85 and 400 K using Au Schottky diodes. The same diodes were used to measure capacitance versus frequency (C - f) characteristics, the temperature dependence of capacitance/conductance for various frequencies (C/G - T), so called admittance spectroscopy,^{31,32} and deep-level transient spectra with optical excitation (ODLTS).^{33,34} We also measured the spectra of deep traps in our heterostructures by photoinduced current transient spectroscopy (PICTS).³⁵ In both techniques a deuterium UV lamp with mechanically actuated shutter was used to produce optical light pulses. PICTS spectra were taken on samples with two In stripes separated by about 5 mm and having no gate between them. This structure imitates drain-source current flow after an optical injection pulse into a gateless HEMT. Experimental setups are described in more detail previously.^{36,37}

III. RESULTS

A. Hall-effect measurements

The room-temperature and 77-K 2DEG concentrations, and mobilities, in the as-grown heterostructure were, respectively, $1.5 \times 10^{13} \text{ cm}^{-2}$ (300 K), $1.2 \times 10^{13} \text{ cm}^{-2}$ (77 K), $800 \text{ cm}^2/\text{V s}$ (300 K), and $1500 \text{ cm}^2/\text{V s}$ (77 K). Some nonuniformity ($\pm 10\%$) in the 2DEG concentration and mobility was observed across the wafer and it was also noticed that the 2DEG concentration was slightly dependent on the surface treatment before measurements (boiling in isopropyl, etching in HCl, and illumination with a deuterium lamp were tried). The highest 2DEG concentrations were consistently observed after etching in HCl and this surface treatment was used as a standard routine before Hall measurements. Because of the slight nonuniformity of electrical properties and because irradiation with different doses of neutrons was done on different pieces cut from the same wafer rather than subsequently on the same piece of material, we felt that it would be more indicative of the changes occurring if the values of the room-temperature and 77-K concentrations, and mobilities, after irradiation with a given dose were normalized to corresponding values measured on the same piece before irradiation.

Figure 2 presents such relative 2DEG 77- and 300-K mobility changes with the neutron dose. The room-temperature mobility starts to decrease appreciably after the dose of 10^{15} cm^{-2} . The 77-K mobility was more sensitive to irradiation and started to decrease after the dose of 10^{14} cm^{-2} . The absolute mobilities after the highest dose of $1.7 \times 10^{17} \text{ cm}^{-2}$ were $90 \text{ cm}^2/\text{V s}$ (300 K) and $160 \text{ cm}^2/\text{V s}$ (77 K).

The changes in the 77- and 300-K 2DEG concentrations are illustrated in Fig. 3. For neutron doses lower than $2.5 \times 10^{16} \text{ cm}^{-2}$ the concentrations slightly increased compared to the preirradiation values, but after irradiation with the dose of $1.7 \times 10^{17} \text{ cm}^{-2}$ the concentrations decreased dramatically by about 40% at room temperature and by about 55% at 77 K.

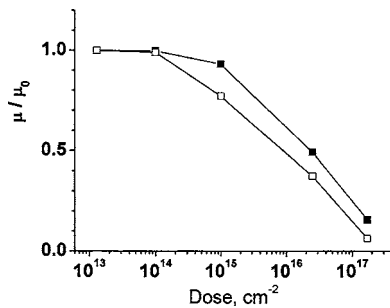


FIG. 2. Changes of AlGaIn/GaN 2DEG mobility μ at room temperature (closed squares) and at 77 K (open squares) after irradiation with fast neutrons; the mobility at each dose is normalized to the value μ_0 measured on a corresponding piece of material before irradiation.

B. C-V and C/G-T measurements

The apparent uncompensated donor concentration in the undoped GaN layer before irradiation was $\sim 10^{16} \text{ cm}^{-3}$ and gradually decreased with increasing dose of irradiation. After irradiation, the measured donor profiles for the low-dose-irradiated sample showed unphysically strong increases near $\sim 0.2 \mu\text{m}$, far away from the interface of the GaN with sapphire. From the actual C-V curves (Fig. 4) it is clear that this artifact is due to the plateau in capacitance at high reverse biases. In normal circumstances, either the thickness corresponding to this plateau would correspond to the total thickness of GaN for high-resistivity GaN layers or the capacitance would not show any plateau for conducting films. Moreover, even if one assumes that there is a highly conducting layer of $0.2 \mu\text{m}$ below the AlGaIn/GaN interface this is difficult to reconcile. The amount of the damage due to neutrons should be uniform throughout the GaN layer and one would expect a jump in concentration around $0.2 \mu\text{m}$ from the interface. The C-V characteristic for the virgin sample in Fig. 4 looks like a leaky metal-insulator-semiconductor (MIS) structure.³⁸ When the sample was cooled to 85 K the capacitance at the negative-bias plateau in C-V became close to the one expected for the GaN film of $3\text{-}\mu\text{m}$ thickness, but the actual value of the “flat-band” voltage³⁸ depended very sensitively on the value of bias at which the sample was cooled down: the higher the negative bias during cooling down, the lower the flat-band voltage. The presence of the plateau precludes extraction of the doping beyond the $0.2\text{-}\mu\text{m}$ depth. The plateau increases in extent with increasing

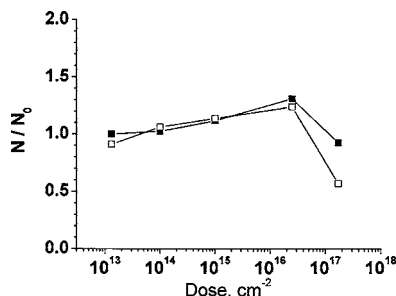


FIG. 3. Changes of AlGaIn/GaN 2DEG concentration N at room temperature (closed squares) and at 77 K (open squares) after irradiation with fast neutrons; the value at each dose is normalized to the value N_0 measured on a corresponding piece of material before irradiation.

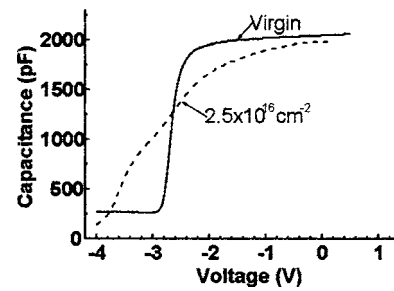


FIG. 4. C-V characteristics measured at room temperature at 1 kHz on the virgin AlGaIn/GaN sample and on the sample irradiated with $2.5 \times 10^{16} \text{ cm}^{-2}$ neutrons.

dose over the entire dose range. In terms of MIS C-V characteristics this would imply that some negative built-in charge was generated. In a recent study of the origin of the gate lag in AlGaIn/GaN HEMTs (Ref. 39) it was shown that the effect is very likely due to tunneling of electrons from the Schottky gate electrode into AlGaIn barrier under high reverse bias. This could also easily be the case for the observed flat-band shifts in our AlGaIn/GaN heterojunctions.

To find the depth of the traps in AlGaIn barrier involved in the process, admittance spectra of the structure at high reverse bias were carried out: the decrease in capacitance with temperature at low temperatures is due to the structure being driven towards stronger depletion as the negative charge is built up in AlGaIn due to tunneling from the Schottky diode metal. The activation energy for the recovery of capacitance/conductance in admittance spectra is then equal to the activation energy for the release of electrons captured by the traps in AlGaIn. In Fig. 5 we show the admittance spectra for the virgin sample. The activation energy for the traps is close to 0.21 eV and quite similar to the activation energy of the traps in AlGaIn responsible for the gate lag.³⁹ If the density of these traps increased with irradiation, this would manifest itself in the stronger shift of the flat-band voltage to positive values. However, for low doses the changes, if occurring, were low and within the accuracy of measurements. For higher doses the C-V characteristics became highly nonideal, as shown for the dose of $2.5 \times 10^{16} \text{ cm}^{-2}$ in Fig. 5. The transition from “accumulation” to “depletion” in terms of MIS C-V characteristics became very broad and generally showed two steps. If the analogy with MIS behavior were to be drawn further this would imply

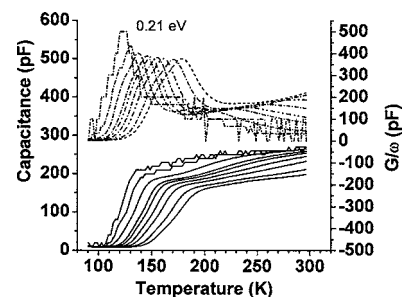


FIG. 5. The temperature dependence of capacitance C (solid curves, left y axis) and of conductance divided by frequency G/ω (dashed curves, right y axis) measured at a high reverse bias of -4 V on the virgin AlGaIn/GaN sample; the measurement frequencies are 100 Hz, 300 Hz, 1 kHz, 3 kHz, 5 kHz, 10 kHz, 20 kHz, 50 kHz, and 100 kHz.

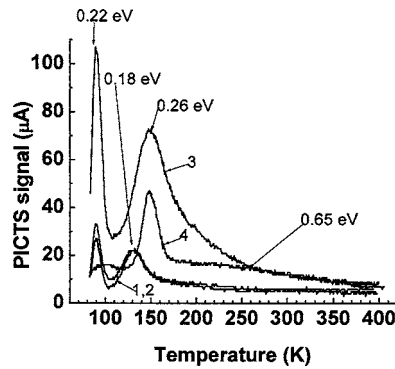


FIG. 6. PICTS spectra measured with ohmic contacts on AlGaIn/GaN samples before irradiation (curve 1), after irradiation with 10^{14} cm⁻² (curve 2), 10^{15} cm⁻² (curve 3), and 2.5×10^{16} cm⁻² (curve 4); measurements conditions: 0.5-V bias, illumination with a 5-s-long D₂ lamp pulse, and time windows of 150 ms/1500 ms.

introduction of high density of deep states either in AlGaIn or at the AlGaIn/GaN interface.³⁸ Assessment of the energy position of corresponding levels is not trivial, but if one assumes that the changes in capacitance with temperature occurring at reverse biases corresponding to the two traps in the C-V curve of Fig. 4 are due to trapping and release of electrons by the states in question, the activation energy determined from admittance spectra should be close to the energy levels of the states in question. These measurements prove to be very time consuming and only preliminary results are available at this moment. The activation energies in question, according to these preliminary measurements, are 0.3 and 0.45 eV. When samples were cooled under bias and returned to room temperature, the current-voltage characteristics were similar as they were before.

C. PICTS and ODLTS measurements

Figure 6 compares the PICTS spectra taken on samples with Ohmic contacts before irradiation and after neutron doses of 10^{14} , 10^{15} , and 2.5×10^{16} cm⁻². All spectra were taken with the bias of 0.5 V. Optical injection led to increased current through the channel and, when analyzing the relaxation curves for this excessive current in the usual fashion,³⁵ two sharp peaks with apparent activation energies of 0.22 and 0.18 eV could be detected in the virgin sample and the 10^{14} -cm⁻² sample. The spectra were virtually the same in both cases. For a higher dose of 10^{15} cm⁻² the amplitude of the 0.22-eV peak was very greatly increased and the activation energy of the second peak increased to 0.26 eV while its magnitude dramatically increased compared to the amplitude of the 0.18-eV peak in the virgin sample. For the highest dose of 1.7×10^{17} cm⁻² the PICTS signal was very much lower than for lower doses, no peaks at 0.22 and 0.26 eV could be detected, the only signal was due to traps with apparent activation energy of 0.6 eV, and deeper traps revealed for longer probing times and characterized by the apparent activation energy of 1 eV (Fig. 7; the results for the highest dose are shown separately to avoid congestion in Fig. 6).

The results of ODLTS spectra measurements are presented in Fig. 8. (DLTS spectra with electrical injection were

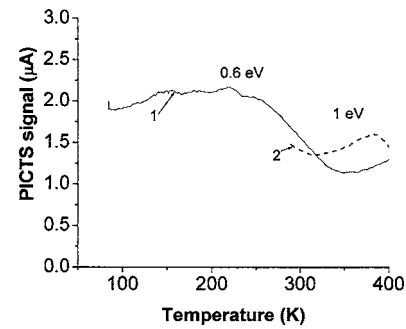


FIG. 7. PICTS spectra measured on the sample irradiated with 1.7×10^{17} cm⁻² neutrons; solid curve: time windows of 150 ms/1500 ms (curve 1), dashed curve: time windows of 1 s/10 s (curve 2).

taken, but showed very low amplitudes of the peaks with high noise level because of problems with series resistance for capacitance measurements at 1 MHz; however, ODLTS spectra could be measured, although the absolute values of concentration cannot be trusted.) In the virgin sample and the sample irradiated with 10^{14} -cm⁻² neutrons, two traps with apparent activation energies very close to the ones observed in PICTS could be detected. During the relaxation the capacitance was decreasing with time, as for the hole-traps-like defects. For the samples irradiated with a higher dose of 2.5×10^{16} cm⁻² the signal was much stronger and the dominant traps, as for the case of PICTS, showed apparent activation energies of 0.26 and 0.6 eV.

IV. DISCUSSION

Consider first the results of 2DEG concentration and mobility measurements shown in Figs. 2 and 3. The decrease of mobility in the channel in Fig. 2 is related to the introduction of additional scattering centers in the GaN layer by neutron irradiation. Understandably, the effect is stronger at low temperatures where the impact of impurity scattering is more pronounced. The results for the 2DEG concentration are more complicated. The value of concentration in the channel is due to two major contributions: (a) the charge coming from strong piezoelectric field and respective band bending,^{1,2} and (b) the charges that, as in usual modulation-doped heterojunctions, are due to tunneling of electrons from the filled centers in AlGaIn to the states in the quantum well near the AlGaIn/GaN interface. The former effect is the dominant one in AlGaIn/GaN.^{1,2} It should not be greatly

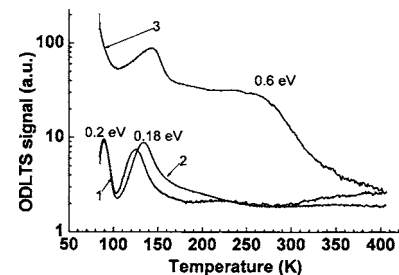


FIG. 8. ODLTS spectra measured on the virgin sample (curve 1), on the sample irradiated with 10^{14} cm⁻² (curve 2), and 2.5×10^{16} cm⁻² (curve 3); measurement conditions: reverse bias -2 V, D₂ lamp pulse of 5 s long, and time windows of 150 ms/1500 ms.

affected by irradiation. The magnitude of the latter effect is determined by the number of states that can participate. It is known that, upon irradiation of GaN and AlGaIn, both relatively shallow states and deeper states are introduced and, at initial stages, the introduction of shallow defects dominates.^{6,7,9} When the deeper defects start to dominate for higher doses the Fermi level in the AlGaIn barrier is shifted deeper toward the band gap and the charge transfer from AlGaIn to GaN becomes less efficient. Consequently, at higher doses the 2DEG concentration rapidly decreases. This picture is qualitatively confirmed by our previously published results of high-Al-content AlGaIn irradiation with protons.¹³ It is important to note that the product μN (where μ is the 2DEG mobility and N is the 2DEG concentration) in AlGaIn/GaN heterojunctions does not change appreciably up to neutron doses of about 10^{15} cm^{-2} , which indicates a high radiation hardness of AlGaIn/GaN HEMTs.

The neutron-irradiation-induced concentration changes in undoped n -GaN depend on the Fermi-level position. The carrier concentration in our virgin n -GaN is $\sim 2 \times 10^{16} \text{ cm}^{-3}$. This decreased to $8 \times 10^{15} \text{ cm}^{-3}$ after irradiation with 10^{14} cm^{-2} neutrons. This suggests an initial carrier removal rate of about 120 cm^{-1} . However, for the high dose of $2.5 \times 10^{16} \text{ cm}^{-3}$ the concentration in the GaN film is about 10^{15} cm^{-3} , yielding a removal rate of only about 0.4 cm^{-1} . This is in general agreement with the published data for irradiated GaN, where it is difficult to achieve high resistivity by high-energy particle irradiation.⁶⁻⁸ If, as it seems more appropriate, the structure in question is considered as a leaky MIS capacitor the absolute values of removal rates will naturally change, but no quantitative estimates have been attempted because of the lack of an accurate theory describing the data.

The PICTS and ODLTS measurements suggest that, upon illumination, both the current through the channel and the capacitance of the structure increase and, once the light is switched off, both decrease with time, as would be the case for hole traps located either in AlGaIn or GaN. The double peaks near 0.18 and 0.2 eV in PICTS and ODLTS spectra of the virgin and lightly irradiated samples likely arise from hole traps in GaN and AlGaIn, respectively. The 0.26-eV hole traps that dominate the spectra of moderately irradiated samples (Figs. 6 and 8) are similar to the traps introduced in p -GaN by proton irradiation.¹¹ This also goes for the 0.6- and 1-eV hole traps detected in heavily irradiated samples.

V. CONCLUSIONS

Measurable changes in 2DEG mobility in AlGaIn/GaN heterojunctions after neutron irradiation start at doses higher than 10^{14} cm^{-2} ; 2DEG concentrations decrease dramatically only after irradiation with the dose of $1.7 \times 10^{17} \text{ cm}^{-2}$. The product μN which is a figure of merit for HEMT performance starts to decrease after a dose of 10^{15} cm^{-2} neutrons. This shows that the radiation hardness of AlGaIn/GaN HEMTs should be higher than for AlGaAs/GaAs counterparts. The observed decrease in mobility is due to the introduction of additional scattering centers in GaN channel. The behavior of the 2DEG concentration is explained by the

neutron-irradiation-induced introduction of relatively shallow centers in AlGaIn, contributing to modulation doping at low doses and by moving of the Fermi level toward the midgap at high doses. C - V characteristics of the AlGaIn/GaN heterostructures studied resemble MIS structures. The shift of the "flat-band" voltage of such structures toward more positive values at high reverse bias upon cooling down is explained by the tunneling of electrons from the Schottky metal into the localized states in the AlGaIn barrier. These states are located 0.21 eV below the conduction band of AlGaIn. These are most likely the same states responsible for the gate-lag effect in AlGaIn/GaN HEMTs. After heavy irradiation the states involved in the process are located at approximately 0.3 and 0.45 eV from the conduction-band edge of AlGaIn.

ACKNOWLEDGMENTS

The work at IRM was supported in part by a grant from the Russian Federation for Basic Research.

- ¹M. S. Shur and M. A. Khan, in *GaN and AlGaIn Devices: Field Effect Transistors and Photodetectors*, GaN and Related Materials II, edited by S. J. Pearton (Gordon and Breach, Netherlands, 1999), pp. 47–92.
- ²S. Rajan, H. Xing, D. Jena, S. P. DenBaars, and U. K. Mishra, *Appl. Phys. Lett.* **84**, 1591 (2004).
- ³M. Linde, S. J. Uffring, G. D. Watkins, V. Harle, and F. Scholz, *Phys. Rev. B* **55**, R10177 (1997).
- ⁴D. C. Look, D. C. Reynolds, J. W. Hemsky, J. R. Sizelove, R. L. Jones, and R. J. Molnar, *Phys. Rev. Lett.* **79**, 2273 (1997).
- ⁵Z.-Q. Fang, D. C. Look, W. Kim, Z. Fan, A. Botchkarev, and H. Morkoc, *Appl. Phys. Lett.* **72**, 2277 (1998).
- ⁶S. A. Goodman, F. D. Auret, F. K. Koschnick, J.-M. Spaeth, B. Beaumont, and P. Gibart, *Mater. Sci. Eng., B* **B71**, 100 (2000).
- ⁷A. Y. Polyakov, A. S. Usikov, B. Theys, N. B. Smirnov, A. V. Govorkov, F. Jomard, N. M. Shmidt, and W. V. Lundin, *Solid-State Electron.* **44**, 1971 (2000).
- ⁸V. V. Emtsev, V. Yu. Davydov, and E. E. Haller, *Physica B* **308**, 58 (2001).
- ⁹M. Hayes, F. D. Auret, L. Wu, W. E. Meyer, J. M. Nel, and M. J. Legodi, *Physica B* **340–342**, 421 (2003).
- ¹⁰D. Haase, M. Schmidt, W. Kremer, A. Dornen, V. Harle, F. Scholz, M. Burkhardt, and H. Schweizer, *Appl. Phys. Lett.* **69**, 2525 (1996).
- ¹¹A. Y. Polyakov, N. B. Smirnov, A. V. Govorkov, S. J. Pearton, J. M. Zavada, and R. G. Wilson, *J. Appl. Phys.* **94**, 3069 (2003).
- ¹²A. Y. Polyakov, N. B. Smirnov, A. V. Govorkov, K. H. Baik, S. J. Pearton, and J. M. Zavada, *J. Vac. Sci. Technol. B* **22**, 2291 (2004).
- ¹³A. Y. Polyakov, N. B. Smirnov, A. V. Govorkov, N. V. Pashkova, S. J. Pearton, J. M. Zavada, and R. G. Wilson, *J. Vac. Sci. Technol. B* **21**, 2500 (2003).
- ¹⁴C.-W. Wang, *J. Vac. Sci. Technol. B* **20**, 1821 (2002).
- ¹⁵B. Luo *et al.*, *Solid-State Electron.* **47**, 1015 (2003).
- ¹⁶B. Luo *et al.*, *Appl. Phys. Lett.* **79**, 2196 (2001).
- ¹⁷B. D. White *et al.*, *IEEE Trans. Nucl. Sci.* **49**, 2695 (2002).
- ¹⁸B. D. White *et al.*, *IEEE Trans. Nucl. Sci.* **50**, 1934 (2003).
- ¹⁹S. M. Khanna *et al.*, *IEEE Trans. Nucl. Sci.* **51**, 2729 (2004).
- ²⁰A. P. Karmarkar, J. Bongim, D. M. Fleetwood, R. D. Schrimpf, R. A. Weller, B. D. White, L. J. Brillson, and U. K. Mishra, *IEEE Trans. Nucl. Sci.* **51**, 3801 (2004).
- ²¹X. Hu *et al.*, *IEEE Trans. Nucl. Sci.* **50**, 1791 (2003).
- ²²X. Hu *et al.*, *IEEE Trans. Nucl. Sci.* **51**, 293 (2004).
- ²³F. Gaudreau, P. Fournier, C. Carlone, S. M. Khanna, H. Tang, J. Webb, and A. Houdayer, *IEEE Trans. Nucl. Sci.* **49**, 2702 (2002).
- ²⁴S. J. Cai *et al.*, *IEEE Trans. Electron Devices* **47**, 304 (2000).
- ²⁵B. Luo *et al.*, *Appl. Phys. Lett.* **80**, 604 (2002).
- ²⁶A. Ionascut-Nedelcescu, C. Carlone, A. Houdayer, H. J. von Bardeleben, J. L. Cantin, and S. Raymond, *IEEE Trans. Nucl. Sci.* **49**, 2733 (2002).
- ²⁷S. M. Khanna, D. Estan, A. Houdayer, H. C. Liu, and R. Dudek, *IEEE Trans. Nucl. Sci.* **51**, 3585 (2004).
- ²⁸S. M. Khanna *et al.*, *IEEE Trans. Nucl. Sci.* **51**, 2729 (2004).

- ²⁹C. Li and S. Subramanian, IEEE Trans. Nucl. Sci. **50**, 1998 (2003).
- ³⁰J. F. Ziegler, J. P. Biersack, and U. Littmark, *The Stopping and Range of Ions in Solids*, 2nd ed. (Pergamon, New York, 1996).
- ³¹L. S. Berman and A. A. Lebedev, *Capacitance Spectroscopy of Deep Defects in Semiconductors* (Nauka, Leningrad, 1981).
- ³²*Identification of Defects in Semiconductors*, edited by M. Stavola (Academic, San Diego, 1998).
- ³³G. M. Martin, A. Mitonneau, D. Pons, A. Mircea, and D. W. Woodard, J. Phys. C **13**, 3855 (1980).
- ³⁴A. Y. Polyakov *et al.*, J. Appl. Phys. **92**, 3130 (2002).
- ³⁵A. Y. Polyakov *et al.*, Appl. Phys. Lett. **83**, 2608 (2003).
- ³⁶A. Y. Polyakov, N. B. Smirnov, A. V. Govorkov, M. G. Mil'vidskii, A. S. Usikov, B. V. Pushnyi, and W. V. Lundin, Solid-State Electron. **43**, 1929 (1999).
- ³⁷A. Y. Polyakov, N. B. Smirnov, A. V. Govorkov, M. Shin, M. Skowronski, and D. W. Greve, J. Appl. Phys. **84**, 870 (1998).
- ³⁸S. M. Sze, *Physics of Semiconductor Devices* (Wiley, New York, 1981).
- ³⁹O. Mitrofanov and M. Manfra, Appl. Phys. Lett. **84**, 422 (2004).